[Geophysical Research Letters]

Supporting Information for

Low dissipation of earthquake energy along faults that follow pre-existing weaknesses: field and microstructural observations of Malawi's Bilila-Mtakataka Fault

Jack N. Williams[a,b], Åke Fagereng[a], Luke N.J. Wedmore[b], Juliet Biggs[b], Hassan Mdala[c], Felix Mphepo[c], Michael Hodge[a]

[a]School of Earth and Environmental Sciences, Cardiff University, Cardiff, UK

[b]School of Earth Sciences, University of Bristol, Bristol, UK

[c]Geological Survey Department, Mzuzu Regional Office, Mzuzu, Malawi]

Contents of this file

Introduction

Figures S1-S5 provide additional context of the geomorphology around the Bilila-Mtakataka Fault, to our field observations, and microstructural analysis.

Table S1 lists the samples on which microstructural analysis was performed, their lithology, and their sampling locality.

Figure S1.

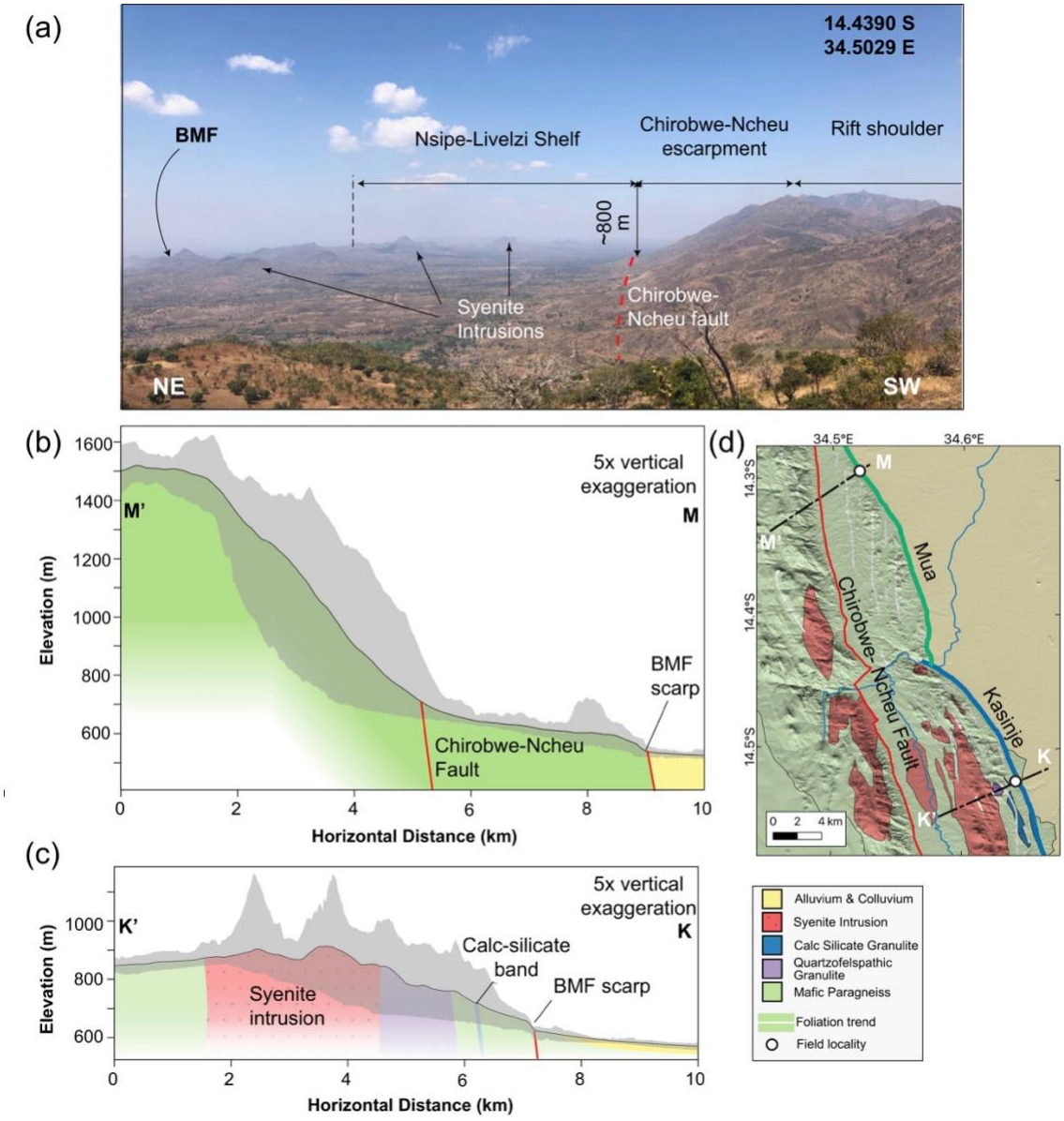

Figure S1: (a) Overview of the Bilila Mtakataka Fault's (BMF) footwall geomorphology taken from the Chirobwe-Ncheu Fault escarpment. See Fig. 1a for location. (b&c) cross sections through the BMF field localities at (b) Mua and (c) Kasinje. Black line and shading represent mean and range of topography in a swath 2.5 km either side of profiles in (d) [Schwanghart & Scherler, 2014]. (d) Map with extent of Mua and Kasinje segments of the BMF and context of cross sections in (b) and (c). Geological units from [Walshaw, 1965] and [Hodge et al., 2018], and are underlain by a TanDEM-X digital elevation model.

Figure S2

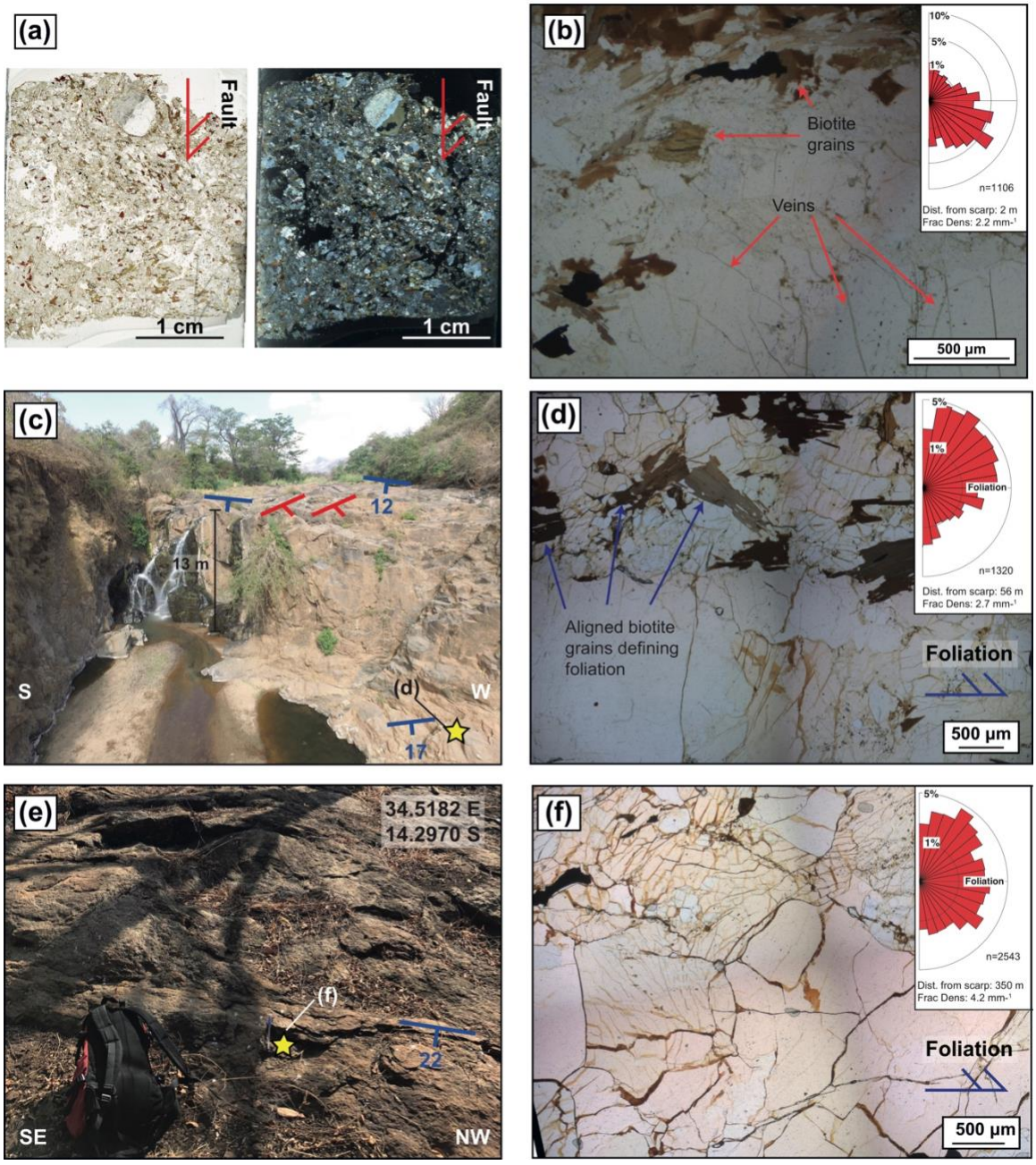

Figure S2: Field and photomicrographs from the BMF exposure at Mua. (a) Thin sections scan in plane polarised and cross polarised light (PPL and XPL respectively) of protocataclasite sample taken adjacent to exposed section of scarp at Mua. (b) Photomicrograph from the sample adjacent to the damage zone in PPL indicating foliation oblique veins in quartzofeldspathic grains. (c) Knickpoint at Mua, which is located beyond the damage zone where joints (blue strike and dip symbols) have >0.1 m spacing, dip moderately to the west, and cross cut the gently dipping foliation (red strike and dip symbols). (d) Photomicrograph in sample from near knickpoint where foliation

oblique veins with fine grained brown fill are still prevalent. (e) Outcrop 350 m from the scarp at Mua where (f) a high density of veins is still observed in thin section. Inset in (c) and (d) are equal area rose plots of fracture segment orientations weighted by length [Healy et al., 2017]. Rose plots and reported fracture densities are for the three sample areas measured in each thin section.

Figure S3

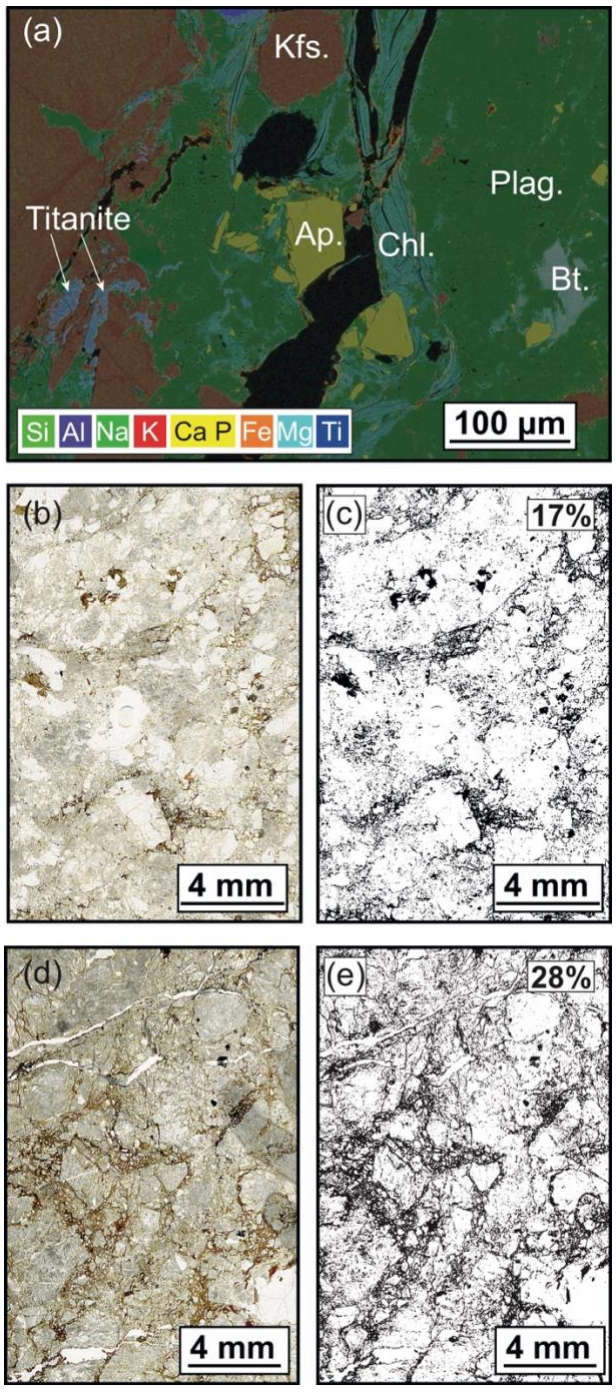

Figure S3: Analysis of matrix in BMF protocataclasites from Mua. (a) False color Energy Dispersive Spectroscopy (EDS) element map with underlain Backscatter Electron Image for area shown in Figure 2d in the main text, in thin section sampled from the Bilila-Mtakataka Fault scarp at Mua. Kfs.; K-feldspar, Plag.; Plagioclase feldspar, Bt.; Biotite, Chl.; Chlorite, Ap.; Apatite. (b) Thin section scan of protocataclasite 0.1 m from scarp. In (c), an image threshold has been applied to (b) using ImageJ, with the dark areas interpreted to

represent cataclasite matrix. The proportion of the image interpreted as matrix using this method is given in the top right of (c). (d&e) Equivalent to (b&c), but for a sample 1 m from the scarp. Note these are upper limits of matrix area, as undeformed biotite grains will be interpreted as matrix.

Figure S4

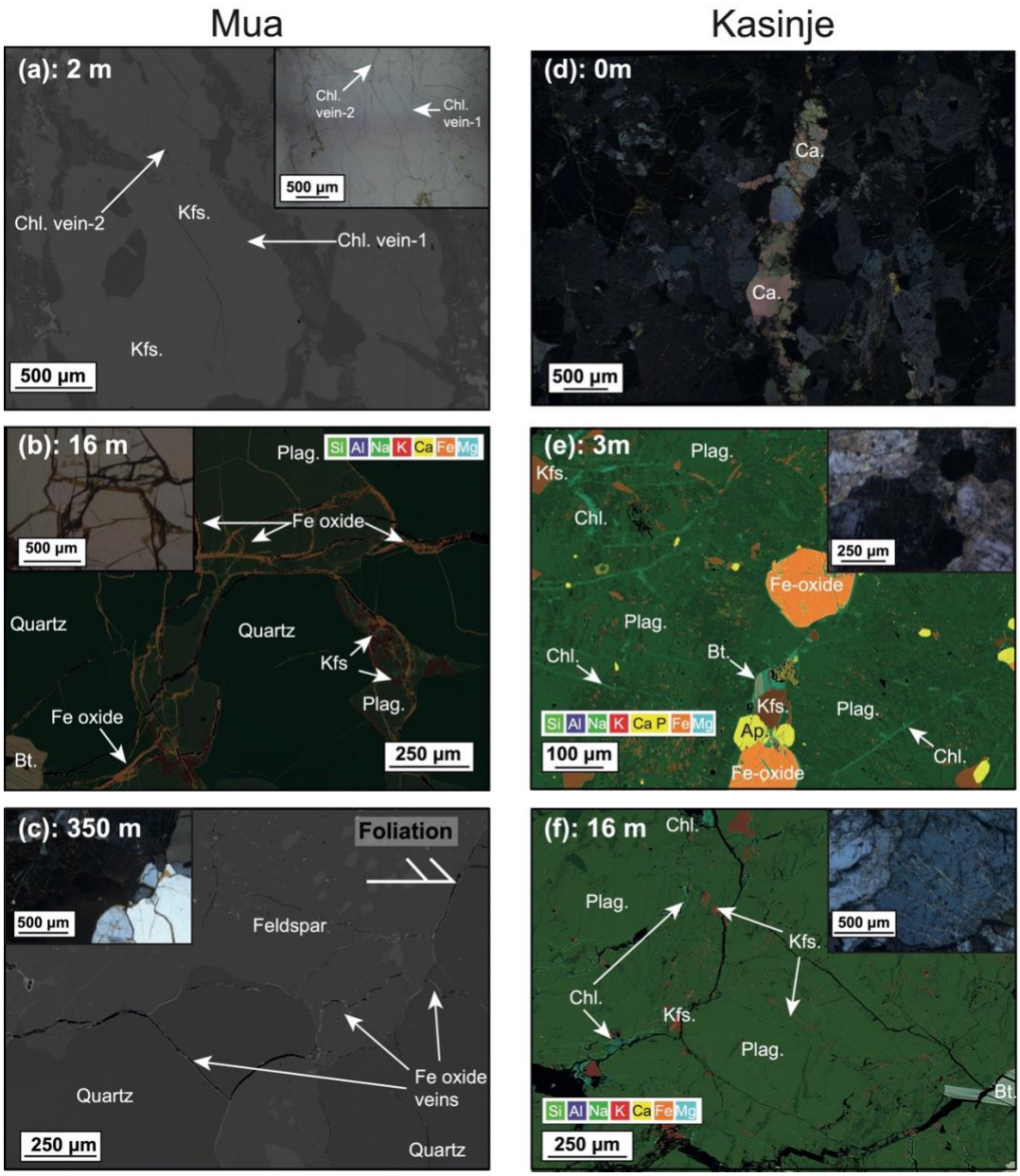

Figure S4: Representative images of microfracture networks around the BMF. Number next to label indicates horizontal distance thin section was sampled from the BMF scarp. Where applicable, insets show photomicrographs from a petrological microscope of the equivalent area in the SEM image. (a) Backscattered electron image (BSE) of chlorite veins in sample 2 m from BMF scarp at Mua (Fig. 2b) where grain-grain contacts are preserved. (b&c) Fe-oxide veins in thin sections from samples at greater distances from the BMF scarp at Mua. (b) is an Energy Dispersive Spectroscopy (EDS) element map underlain by BSE image and (c) is a BSE image. (d) Calcite veins adjacent to the BMF scarp at Kasinje in photomicrograph taken in XPL. (e&f) EDS element maps underlain by BSE image highlighting chlorite veins in samples of (e) footwall and (f) hanging wall

country rock at Kasinje. Interpretation of vein fills in (a) and (c) from EDS point spectra. Kfs.; K-feldspar, Plag.; Plagioclase feldspar, Bt.; Biotite, Chl.; Chlorite, Ca.; Calcite, Ap.; Apatite.

Figure S5

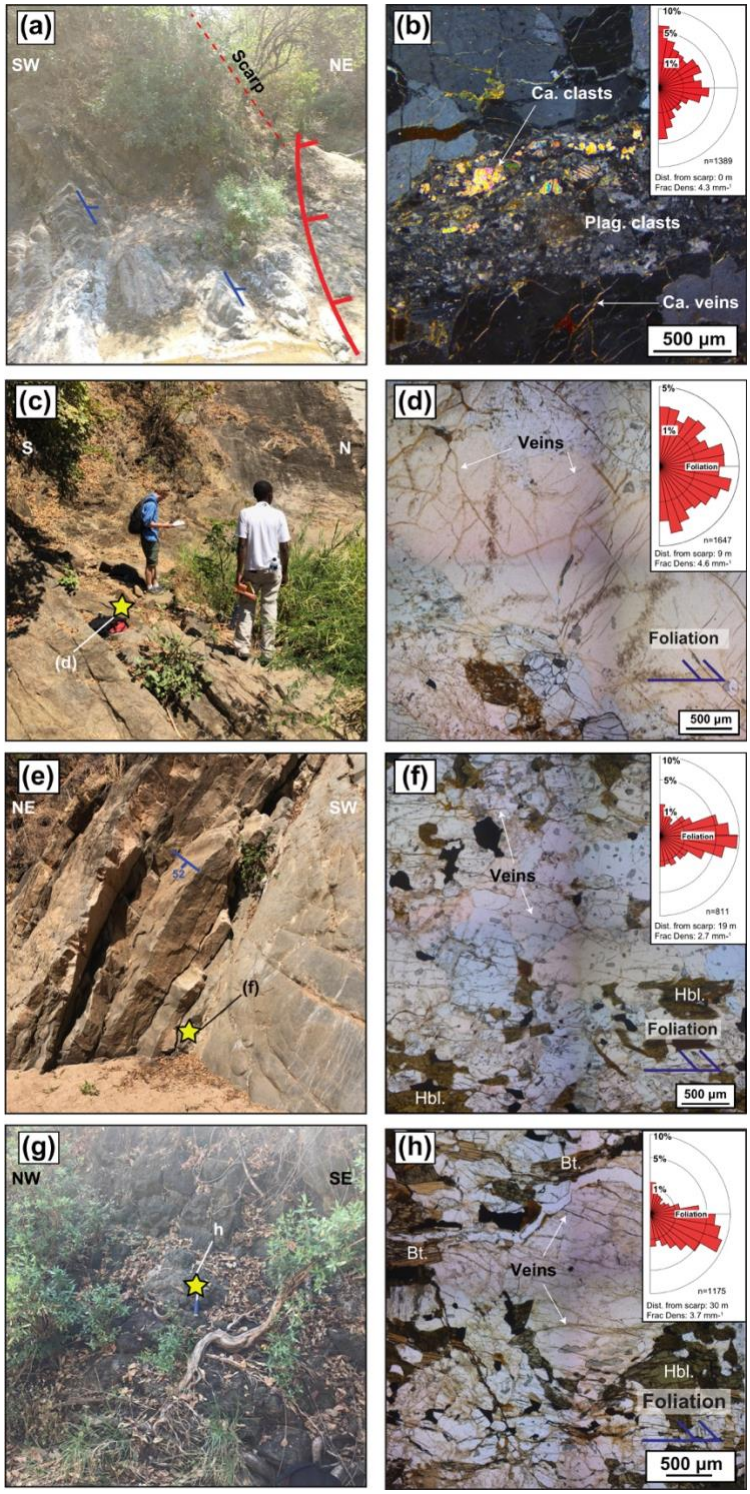

Figure S5: Field and micrographs of BMF exposure at Kasinje. For context of figures localities, see Fig. 3a in the main text. (a) Exposure adjacent to the BMF scarp with closely spaced foliation parallel joints. (b) Sample adjacent to scarp with fragmented calcite and

plagioclase clasts taken in XPL. (c) Footwall exposure adjacent to the BMF damage zone at Kasinje show location of (d), photomicrograph taken in PPL of oblique veins with fine-grained brown fill in weakly foliated migmatic gneiss. (e) Exposure at base of Kasinje knickpoint with foliation parallel joints. Also shown is location of thin section in (f) where veins are aligned to the foliation. (g) Exposure in hanging wall of the BMF showing context of (h) with foliation parallel veins. Reported fracture densities and rose plots in (d), (f), and (h) are for fracture segment orientations weighted by length as in Figs S2.

Table S1. Samples used in microfracture density and Scanning Electron Microscope (SEM) analysis

Sample	Distance from BMF scarp (m)*	Longitude (E)	Latitude (S)	Lithology	Fracture density (mm^{-1})†	SEM analysis
Mua						
MBMF19-03	0.1	34.5204	14.2941	Protocataclasite	$3.2^{+2.1}_{-1.4}$	EDS point spectra & mapping
MBMF18-02	1	34.5204	14.2941	Protocataclasite	$1.7^{+0.5}_{-0.3}$	
MBMF18-03	2	34.5204	14.2941	Biotite gneiss	$2.2^{+0.7}_{-0.8}$	EDS point spectra
MBMF18-04	8	34.5204	14.2941	Biotite gneiss	$3.3^{+1.5}_{-1.0}$	
MBMF18-05	16	34.5204	14.2941	Biotite gneiss	$3.2^{+0.6}_{-0.7}$	EDS point spectra & mapping
BMF1-2	17	34.5204	14.2941	Biotite gneiss	$2.0^{+0.4}_{-0.3}$	
MBMF18-06	56	34.5199	14.2946	Biotite gneiss	$2.7^{+0.5}_{-0.9}$	
MBMF18-07	120	34.5195	14.2950	Biotite gneiss	$0.8^{+0.3}_{-0.2}$	
MBMF19-01	160	34.5193	14.2950	Biotite gneiss	$2.7^{+0.4}_{-0.3}$	
MBMF19-02	215	34.5188	14.2952	Biotite gneiss	$1.4^{+0.3}_{-0.3}$	
MBMF18-08	350	34.5182	14.2970	Biotite gneiss	$4.2^{+1.2}_{-1.4}$	EDS point spectra
Kasinje						
BMF4-4	0.1	34.6410	14.5244	Altered gneiss	$4.3^{+0.8}_{-0.5}$	EDS point spectra
K18-04	3	34.6410	14.5244	Migmatic gneiss	$2.4^{+0.3}_{-0.4}$	EDS point spectra & mapping
K18-03	9	34.6410	14.5244	Migmatic gneiss	$4.6^{+1.1}_{-0.9}$	
K18-06	16	34.6410	14.5244	Altered gneiss	$3.4^{+0.9}_{-0.4}$	EDS point spectra & mapping
K18-01	19	34.6408	14.5245	Hornblende-biotite gneiss	$2.7^{+0.6}_{-0.6}$	
K18-07	30	34.6413	14.5244	Quartzofeldspathic gneiss	$3.7^{+0.4}_{-0.3}$	
K18-08	62	34.6418	14.5250	Hornblende-biotite gneiss	$1.2^{+0.1}_{-0.1}$	

Note. *Measured as distance between sample and fault scarp along a horizontal line perpendicular to fault scarp. Distances <10 m, measured in field with tape measure, distances >10 m measured based on handheld GPS locations with an accuracy of 3-5 m. †Area-weighted average microfracture density for the three sample areas measured within each sample [*Wedmore et al.*, 2020]. Plus and minus values represent range of fracture densities over the three sample areas.